Materials Research Bulletin 153 (2022) 111899

Contents lists available at ScienceDirect

Materials Research Bulletin

journal homepage: www.elsevier.com/locate/matresbu

Research Papers

Bioactive phosphate glass-based fiber with green persistent luminescence

A. Lemiere [a], A. Szczodra [b], S. Vuori [c,d], B. Bondzior [a,e], T.W. Hawkins [f], J. Ballato [f], M. Lastusaari [c], J. Massera [b], L. Petit [a,*]

[a] Photonics Laboratory, Tampere University, Korkeakoulunkatu 3, Tampere 33720, Finland
[b] Faculty of Medicine and Health Technology, Tampere University, Korkeakoulunkatu 3, Tampere 33720, Finland
[c] Department of Chemistry, University of Turku, FI-20014 Turku, Finland
[d] University of Turku Graduate School (UTUGS), Doctoral Programme in Physical and Chemical Sciences, Turku, Finland
[e] Institute of Low Temperature and Structure Research Polish Academy of Sciences, Okólna 2, 50-422 Wrocław, Poland
[f] Department of Materials Science and Engineering, Clemson University, Clemson, SC 29634 United States of America

ARTICLE INFO

Keywords:
Glass
Composite
Fiber
Persistent luminescence
Corrosion

ABSTRACT

The first biophotonic composite fiber with green persistent luminescence is reported. The composites were drawn from preforms prepared by remelting a bioactive glass with commercial persistent luminescent microparticles ($SrAl_2O_4$:Eu^{2+},Dy^{3+}). The duration of the remelt step should be as short as possible to limit the decomposition of the micro-phosphors during glass preparation, as evidenced using electron microscopy coupled with elemental analysis. The presence of the phosphors in the glass inhibits the drawing of fibers with diameter below about 400 μm. Although the drawing process induces some changes in the Eu^{2+} ions' local structure in the phosphors, the fibers still exhibit green afterglow. Despite the presence of the phosphors, the fiber still maintains its bioactive response, as characterized by the release of ions from the glass to the environment and the successive precipitation of a reactive layer within a dicalcium phosphate dehydrate composition.

1. Introduction

Since the first bioactive glass in 1971, [1] which was defined as a glass which bonds to bone after implantation in the human body, a large number of bioactive glasses with various compositions have been developed for wide ranging biomedical applications, especially as small, flexible fibers. Indeed, bioactive fibers have found applications in nerve and respiratory sensors, for the monitoring of repetition of movement in muscles, ligaments, and joints articulation by monitoring micro-bend loss, for examples [2] and as reinforcement in fully resorbable composite screws or plates. However, a major limitation with bioactive glasses, including fibers, is their imaging post-operation as these glass-based materials generally exhibit radio-opacity similar to the cortical bone [3]. For the past few decades, in-vivo imaging has been based on fluorescence [4], especially using phosphors with persistent luminescence (PeL) [5]. PeL is defined as an optical emission that lasts from seconds to hours after irradiation source is stopped [6]. One of the most efficient PeL phosphors is $SrAl_2O_4$:Eu,Dy, the afterglow from which can last up to 20 h [7].

Glasses with this phosphor have been prepared successfully using, for example, the "Frozen sorbet method" [8]: a thermal treatment is used to nucleate and grow $SrAl_2O_4$:Eu^{2+},Dy^{3+} crystals in glass in the SrO-Al_2O_3-B_2O_3 system. However, this glass is not bioactive and the technique cannot be applied to prepare bioactive glasses not only with specific composition but also with persistent luminescence as the crystals grow using the chemical components from the glass. The other technique to prepare glasses with persistent luminescence, independently of their composition, is the direct doping method [9]. In this approach, the persistent luminescent particles are introduced into the glass melt. To control the decomposition of the PeL particles during glass preparation, the doping parameters (doping temperature and dwell time) need to be optimized as explained in Ref. [10]. This method has allowed the preparation of glasses in silicate, phosphate and tellurite systems with persistent luminescence [11,12].

Silicate glasses such as 45S5 (46.1 SiO_2 - 26.9 CaO - 24.4 Na_2O - 2.6 P_2O_5, in mol%) and S53P4 (53.8 SiO_2 - 21.8 CaO - 22.7 Na_2O - 1.7 P_2O_5, in mol%) are well known bioactive glasses [13,14]. However, fibers cannot be drawn from these glasses due to their rapid crystallization [15]. Thus, bioactive glasses in systems other than silicates have been under study with phosphate system being good alternative [16,17].

* Corresponding author.
E-mail address: laeticia.petit@tuni.fi (L. Petit).

https://doi.org/10.1016/j.materresbull.2022.111899
Received 31 January 2022; Received in revised form 11 May 2022; Accepted 13 May 2022
Available online 16 May 2022

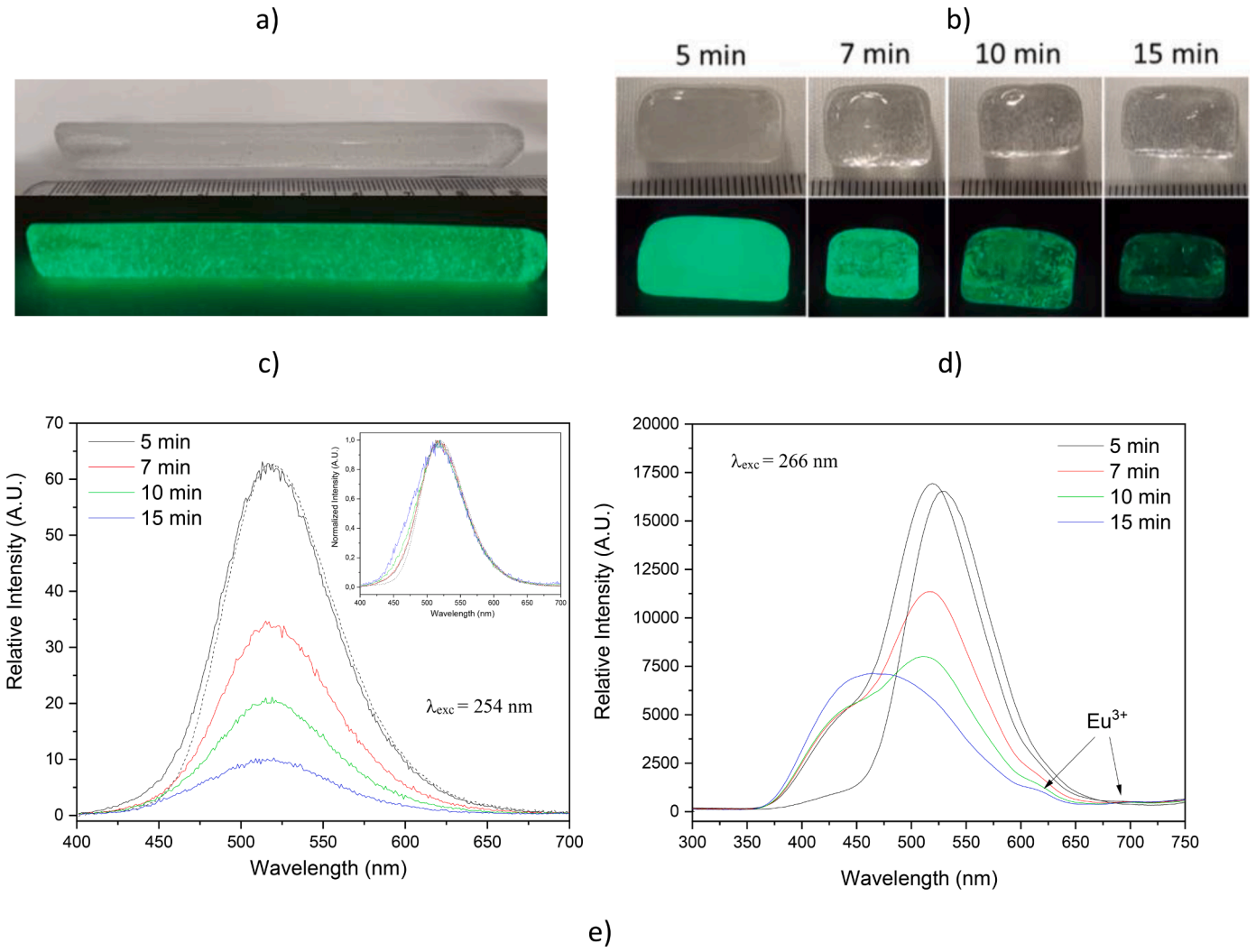

Fig. 1. Picture in daylight and after stopping the UV irradiation of the preform prepared using the direct doping method (a) and of the glasses obtained by remelting glasses with PeL particles using different melting duration (b). Persistent luminescence (c) and conventional luminescence (d) spectra of the glasses prepared using different melting duration (dash line are the PeL and PL spectra of the PeL particles alone, normalized to the spectra of the 5 min remelted glass).

Compared to silicates, phosphate glasses can readily be fabricated at lower melting temperatures. Further, the compositions of phosphates can be easily modified so that the glasses exhibit controlled bioresponse, chemical durability, and improved optical properties [18,19]. More importantly, phosphate glasses with P_2O_5 content greater than 45 mol% are known for their good thermal stability allowing them to be drawn into fiber [20,21]. Phosphate glass with the composition $50P_2O_5$–40SrO-$10Na_2O$ (mol%) was successfully drawn into fibers using a melt–draw spinning process [22] and also from preforms [19]. Persistent luminescence from this glass was obtained by inclusion of phosphors such as the $SrAl_2O_4:Eu^{2+},Dy^{3+}$ particles into the melt [10]. To limit the corrosion of the phosphors to maximize intense and uniform green PeL, the glass was cast 5 min after adding the phosphor into the melt at 1000 °C [10]. To the best of our knowledge, there is no study reporting on the drawing of composite bioactive fibers made of bioactive glass and persistent luminescent phosphors.

Demonstrated here is the ability to draw fiber with persistent luminescence directly from bioactive preforms, which is an important advancement in the scalability of bioactive and persistent luminescent fibers. The drawing and spectroscopic properties of these new biophotonic fibers are reported. The impact of the drawing process on the corrosion of PeL particles is discussed as well as the impact of the addition of the PeL particles on the bioresponse of the glass.

2. Experimental section

2.1. Composite fabrication

Uncoated optical fibers with the composition of $50P_2O_5$–40SrO-$10Na_2O$ (in mol%) were drawn from preform using a custom 6.5 m tall fiber drawing tower. The preform was obtained using the standard melt-quenching process. Glass batches of 25 g were melted at 1050 °C in a silica crucible for 1 h using $NaPO_3$ (Alfa Aesar, tech.), $SrCO_3$ (Sigma-Aldrich, ≥99.9%) and $(NH_4)_2HPO_4$ (Sigma-Aldrich, >98%). The last 2 were mixed and heat treated up to 850 °C to prepare $Sr(PO_3)_2$. Preforms were prepared using the direct doping method whereby the melt was quenched into a cylindrical mold, preheated to 250 °C, 5 min after adding 0.2 wt% of commercial $SrAl_2O_4:Eu^{2+}$, Dy^{3+} microparticles (BG-01, Jinan G.L. New Materials, China) into the melt, which was held at 1000 °C as in Refs. [10,11]. Preforms were also prepared by remelting at 950 °C for 5 to 15 min the glass, crushed into powder (cullet), mixed with 0.2 wt% of $SrAl_2O_4:Eu^{2+},Dy^{3+}$particles. One should mention that 5 min was the shortest time allowing the melting of the batch. Finally, the preforms were annealed at 400 °C for 6 h to release internal stress from the quench. The diameter and the length of the preforms were 10 and ~90 mm, respectively. After annealing and prior to drawing, the preforms were polished. The drawing temperature was 535 °C. Using a feed

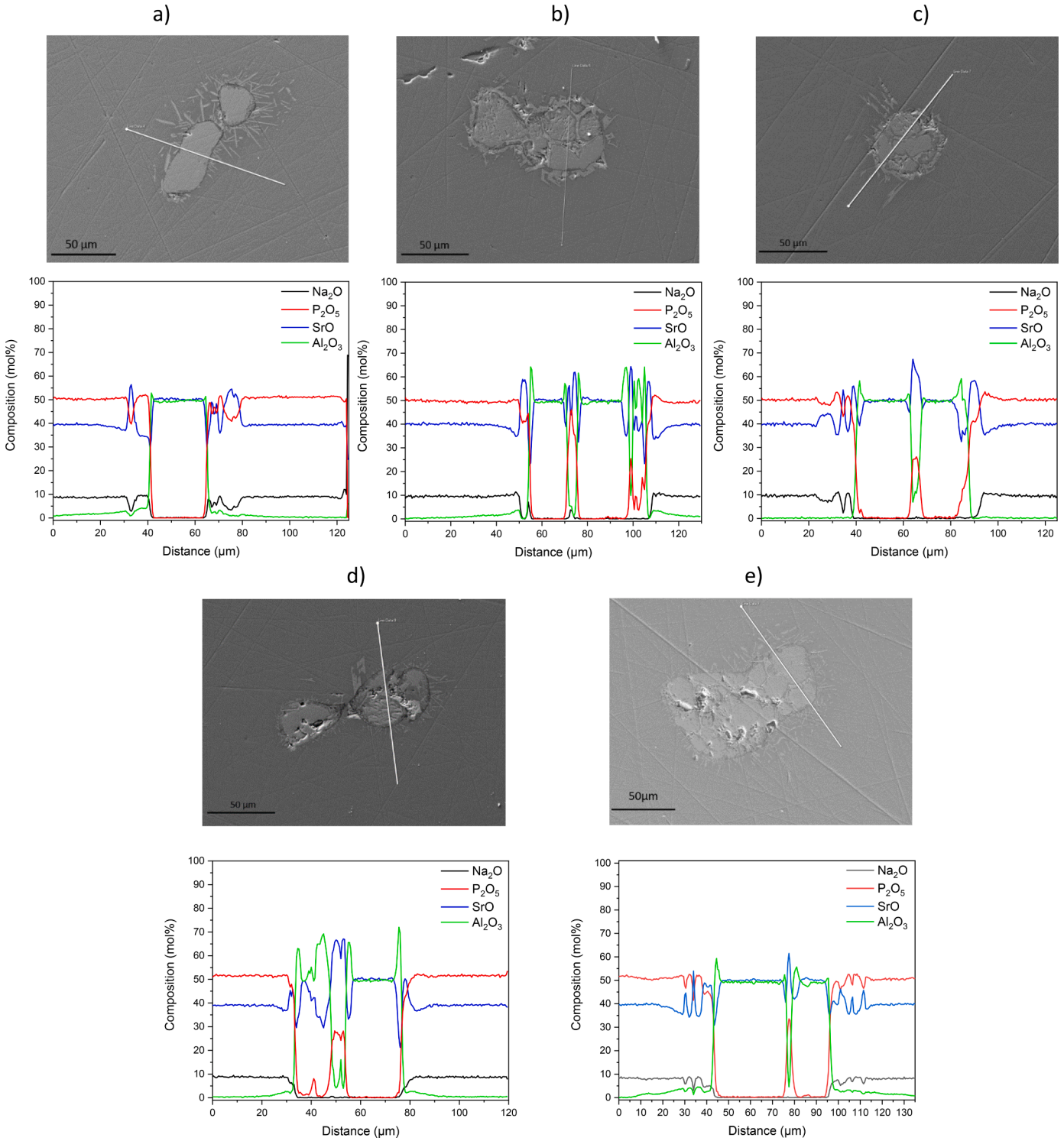

Fig. 2. SEM images and SEM/EDS line profiles giving the elemental distribution across the diameter of a PeL particle found in glasses remelted for 5 (a), 7 (b), 10 (c) and 15 (d) min and in fiber (e). The direction of scan starts at circle (corresponding to 0 µm).

speed of ~1 mm/min and the draw speed of ~6 m/min, 9 m of 400 µm diameter fiber was obtained. The fibers were drawn under nitrogen.

2.2. In-vitro testing

After drawing, the fibers were immersed in simulated body fluid (SBF), prepared as per the protocol described in Ref. [23] for up to 14 days. The pH of the fiber-containing SBF solution was measured over time using a Mettler Toledo SevenMulti™ pH/conductivity meter with an accuracy of ± 0.02 pH units and compared to a solution containing only SBF (labeled as blank solution). 1 ml of the immersion solution was pipetted and diluted in 9 ml ultra-pure HNO_3.

2.3. Characterization

The PeL particles found at the surface of the glass-based materials

(bulk, preforms, and fibers) after polishing as well as the fiber surface post immersion in SBF, were imaged and their composition analyzed using a scanning electron microscope (SEM, Carl Zeiss Crossbeam 540) equipped with Oxford Instruments X-Max^N 80 energy dispersive spectroscopy (EDS) detector. The accuracy of the elemental analysis was ± 1.5 mol%.

An optical microscope (ZEISS Axioscope 5) was used to visually image the fibers and measure their dimensions (at ± 2 μm).

Photoluminescence (PL) spectra were collected using a CCD camera (Avantes, AvaSpec HS-TEC) and Nd:YAG pulse laser (λ_{exc}: 266 nm, 8 ns, TII Lotis). The PeL spectra of the glass prior to and after drawing were collected using a Varian Cary Eclipse Fluorescence Spectrophotometer equipped with a Hamamatsu R928 photomultiplier (PMT). An ultraviolet (UV) lamp (UVLS-24, 4 W, λ_{exc}: 254 nm) was used to excite the samples for 1 min before collecting their PeL spectra. All measurements were performed at room temperature. For the PeL fading measurements, the samples were irradiated for 5 min with a 254 nm hand-held UV-lamp (UVGL-25). The PeL fading curves were obtained by measuring the luminance every 1 s starting 5 s after stopping the excitation using a Hagner ERP-105 luminance meter coupled with a Hagner SD 27 detector. The time taken for the PeL luminance to decay down to 0.3 mcd/m^2 is referred to as the PeL decay time. The accuracy of the decay time was determined from the noise level of each individual measurement.

ICP-OES was performed using a 5110 ICP-OES (Agilent Technologies) to estimate the ion concentration in the solution, post-dissolution.

3. Results and discussion

3.1. Preform fabrication

To prepare biophotonic fibers with strong persistent luminescence, it is crucial to prepare preforms with an appropriate amount of PeL particles, which depends on the composition and size of the particles. This amount of PeL particles should be high enough so that the PeL can easily be observed from the thin fiber. At the same time, the amount of PeL particles should be limited to avoid the formation of PeL agglomerates and also of crystals in the glass as partial crystallization of bioactive glasses has been reported to have a harmful impact on their bioresponse [24]. One should remind that the PeL $SrAl_2O_4$:Eu^{2+},Dy^{3+}particles were reported to act as nucleation agents in some phosphate glasses leading to heterogeneous crystallization with the precipitation of crystals at the glass-PeL particles interface [25]. Additionally, the PeL particles should be homogenously dispersed in the preform to allow the drawing of fibers with homogeneous PeL.

Here, the direct doping method was used to prepare persistent luminescent glasses. 0.2 wt% of the commercial $SrAl_2O_4$:Eu^{2+}, Dy^{3+}particles with micrometer diameter were added in the melt of the glass with the composition $50P_2O_5$–40SrO-$10Na_2O$ (in mol%) which was held at 1000 °C as in Ref. [10]. As shown in Fig. 1a, green PeL can be observed from the preform which is a clear evidence of the survival of the PeL particles. The amount of PeL particles in the glass seems to be appropriate as strong green PeL can be seen from the preform. However, small agglomerates of PeL particles can also be seen in the preform.

To reduce the amount and size of the agglomerates in the large volume of glass, a new preform fabrication method was developed. In this new approach, the phosphate glass was first melted using standard melting process; after quenching, the glass was crushed into powder and remelted with 0.2 wt% of the PeL particles, the remelting step allowing the use of a lower temperature than the one used to originally melt and homogenize the bulk glass from the component crystalline powders. As seen in Fig. 1b, the glasses exhibit intense and uniform green afterglow confirming the survival of the PeL particles during the remelt process. However, the long remelt step leads to afterglow with low intensity (Fig. 1b). As explained in Refs. [10,11], the decrease in intensity of the afterglow when remelting the glass for a long time can be related to the corrosion of the PeL particles, which can be evidenced by the changes in the PeL and PL emission bands after inserting the PeL particles in the glass, as depicted in Figs. 1c and d, respectively. Indeed, the PeL spectra show the typical emission band at 520 nm related to the $4f^65d^1 \rightarrow 4f^7$ transition in Eu^{2+} [26]. The spectral shape of this emission band becomes different with the appearance of a shoulder at ~465 nm as the remelt step is longer revealing that the distribution of the Eu^{2+} ions sites in the phosphors is impacted by the melting process. The PL spectra exhibit 2 bands located at 430 and 525 nm, which are related to the emission of Eu^{2+} in two different cation sites in the PeL $SrAl_2O_4$ particles in agreement with [26]. Changes in the duration of the remelt step leads to changes in the intensity of these emission bands confirming that the sites of Eu^{2+} in the PeL particles change after adding the phosphors in the glass matrix due to the corrosion of the PeL particles occurring during the remelt process. Two bands, with weak intensities, can also be seen at ~610 and 700 nm in the PL spectra presented in Fig. 1d and are associated with the emission of Eu^{3+} [27]. During long remelt process, species from the PeL particles diffuse into the glass, specially Eu^{2+} ions which then oxidize to Eu^{3+} ions.

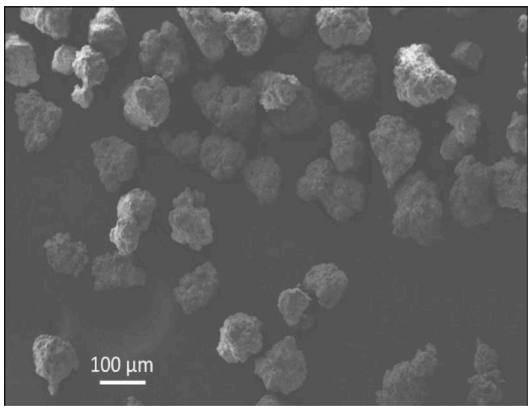

Fig. 3. SEM image of the as-received PeL particles.

The progressive corrosion of the PeL particles with the increase in the duration of the remelt step is confirmed using SEM coupled with EDS. SEM was used to image the PeL particles located at the surface of the glasses. Figs. 2 show SEM images and EDS line profiles of phosphor particles located at the surface of the polished glasses. The size of the particles is at ~40–50 μm, independently of the duration of the remelt step and is similar to the size of the as-received PeL particles (Fig. 3). The composition of the PeL particles embedded in the glasses, when measured in their center, is similar to that of the as-received particles and corresponds to $SrAl_2O_4$. The progressive decomposition of the PeL particles during the remelt step can be evidenced by the appearance of an outer layer at the phosphor-glass interface which is rich in Al_2O_3 rich, as in Refs. [10,27]. The concentration of Al_2O_3 in this layer increases when using long remelt times. Al_2O_3 was also detected in the glasses, confirming the decomposition of the PeL particles during the glass preparation. Finally, Sr rich crystals can be seen at the particles-glass interface and are thought to form in the glass matrix due to the diffusion of Al and Sr from the PeL particles into the glass as explained in Ref. [10]. Based on the spectroscopic properties of the remelted glasses, the preform should be prepared using a short melting process to limit the decomposition of the PeL particles during the remelt step.

3.2. Fiber drawing

Here, the preform was prepared using a 7 min remelt step as a gray coloration of the glasses was observed when using a 5 min remelt step. The preform exhibits strong and uniform PeL as seen in Fig. 4a. Fibers with a diameter of 125 μm were originally planned but, due to the presence of the PeL particles, fibers kept breaking during drawing at these small dimensions. In order to successfully draw fibers, the

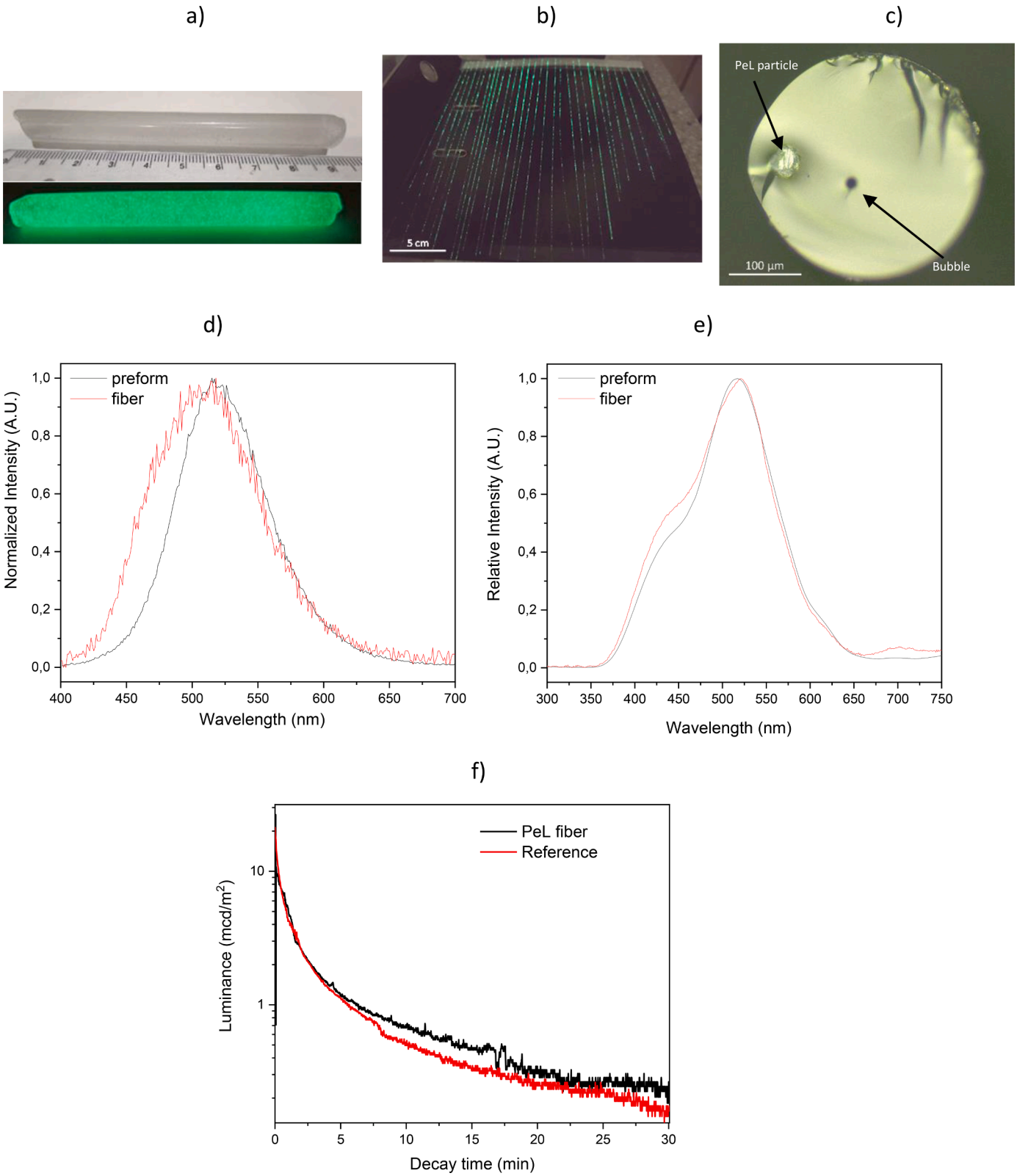

Fig. 4. Pictures in daylight and after stopping the UV irradiation of the preform obtained by remelting the glass with the PeL particles for 7 min (a) and of the resulting fibers (b). Optical image of the fiber cross-section taken with 10x objective (c). PeL (d) and PL (e) spectra of the preform and fiber. PeL fading curve of the fiber and of a Al_2O_3 powder mixed with 0.2 wt% of PeL particles, used as a reference. The samples were irradiated for 5 min with a 254 nm (f).

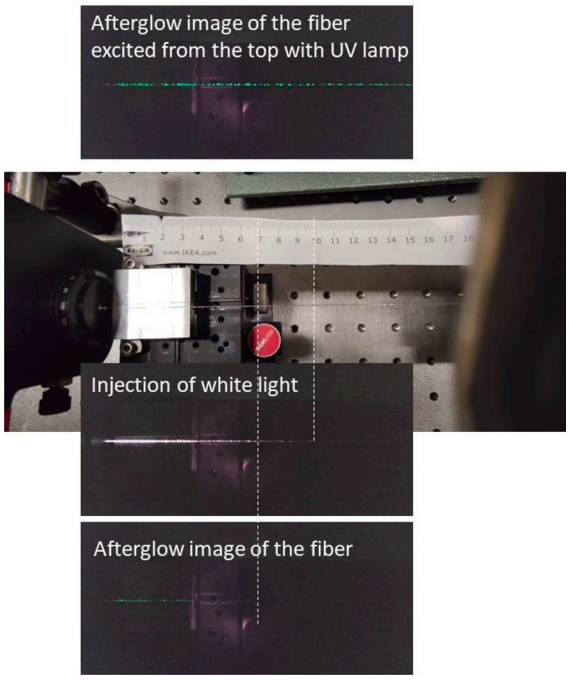

Fig. 5. Optical setup showing the white light injected into the fiber and the corresponding green afterglow from the fiber.

diameter of the fiber was increased to 400 μm. It is worth noting that the fibers were drawn without any polymer layer to allow the investigation of their bioresponse when immersed in SBF.

Fig. 4b shows the afterglow images of the fibers. Fibers exhibit green PeL confirming the survival of the PeL particles during the drawing process. The presence of the PeL particles in the fiber could also be confirmed using an optical microscope (Fig. 4c) and SEM (Fig. 2e). The presence of the PeL particles with micrometer size in the fiber modifies the shape of the fiber (Fig. 4c). As shown in Fig. 4d and e, the shape of the PeL and PL bands changes after drawing process indicating that the drawing process at 535 °C has an impact on the PeL particles embedded in the glass. The absolute emission intensity and the afterglow fading curve were measured after 5 min irradiation at 254 nm (Fig. 4f). The measurement was done for the fibers and for a powder prepared from Al_2O_3 mixed with the PeL particles (0.2 wt% corresponding the weight percentage in the fibers) used as reference. For the measurement, only a rectangular part of the detectable circular sample area was filled with one layer of fibers placed as close to each other as possible. The obtained signal was then corrected based on the area of this rectangle versus that of the circular total area. There are some uncertainties in the definition of the true area covered by the fibers, because of the difficulty in aligning them next to each other. Nevertheless, the absolute PeL emission intensity of the fiber at the beginning of the PeL fading is 15 mcd/m^2 which is similar to the reference powder (21 mcd/m^2). The PeL decay time of the fiber is (20 ± 1) min which is similar to that of the diluted PeL particles powder measured at (17 ± 1) min. It is clearly shown from the spectroscopic properties of the PeL fiber that although drawing fiber from a bulk preform is a rapid process, the drawing process still induces small changes in the sites of the Eu^{2+} ion. These changes in the site of Eu^{3+} are too small to impact the PeL performance of the PeL particles during the fiber drawing process.

The fiber was first excited with a UV lamp from above to excite and locate the PeL particles in the fiber. Then a laser diode (Oceans Insight DH-mini, 200–2500 nm, ~19 μW) was injected in a ~30 cm long fiber segment to determine the distance the light can propagate inside the fibers. As shown in Fig. 5, the white light from the diode propagates over 10 cm in the fibers. After 30 s of white light injection in the fiber, the PeL particles can be visually observed from their afterglow up to 7 cm from the light input.

3.3. *In-vitro testing*

The PeL fibers were immersed in SBF for up to 14 days. Although the fibers appear to be covered with a reactive layer after immersion in SBF, green PeL can still be seen from these fibers (Fig. 6a). The change in pH (respective to the blank) is presented in Fig. 6b. As expected, when phosphate glasses with a metaphosphate structure are immersed in SBF [28], the change in pH is moderate over time. The slight decrease in pH can be assigned to the large release of phosphorus ions, as described in Refs. [28,29]. The ions released from the glass was assessed using inductively coupled plasma - optical emission spectrometry (ICP-OES, Fig. 6c). The ions release is presented respectively to the initial P, Ca, Sr and Mg in the blank SBF solution. In one hand, phosphorus and strontium ions are being released into the solution whereas, on the other hand, calcium and magnesium ions are being consumed. This is related to the formation of a reactive layer [29]. The consumption of Mg also indicates that part of the Mg from the solution is being incorporated into the reactive layer. It should be noted that no aluminum ions were found in the dissolution solution indicating minimal hydrolytic degradation of the PeL particles. The presence of the reactive layer was confirmed using SEM. As depicted in Fig. 6d, the fiber surface becomes rough after 14 days in SBF. Not only does the diameter of the fiber decrease from 400 to ~310 μm, but a ~30 μm thick layer can be seen at the surface of the fiber. This layer was found to be fragile as it easily detached from the fiber when preparing the SEM samples. The composition of the layer was analyzed using EDS. As summarized in Table 1, Ca, Mg, K and Cl (from the SBF solution) and Sr were found. The (Ca+Mg+Sr)/P ratio was ~1.5 confirming the precipitation of a dicalcium phosphate dehydrate (DCPD) layer, in which the Ca can be partially substituted by Sr and/or Mg. As explained in Ref. [28], it is the release of P during the dissolution of the fiber which leads to the supersaturation of the SBF and so to the precipitation of the DCPD layer. Worth noting is that traces of Al were also found in the layer revealing that the components from the PeL particles also participate in the formation of the reactive layer. Overall, the dissolution of the fibers study indicates that the fiber drawing and the presence of the PeL particles does not inhibit the glass bioactivity confirming that it is possible to prepare bioactive fiber with green persistent luminescence.

4. Conclusion

In summary, the first bioactive phosphate glass-based fibers with green persistent luminescence were successfully drawn from preform. The green persistent luminescence was obtained by embedding into the glass matrix the commercial $SrAl_2O_4:Eu^{2+},Dy^{3+}$ phosphors. To obtain a 10 cm long preform with homogeneous and intense green afterglow, the phosphors should be mixed into the glass crushed into powder before remelting the glass-PeL particles mixture. The remelting of the glass allows the use of lower temperature than that needed to initially melt the precursors used to prepare the glass. To limit the decomposition of the phosphors during glass preparation, the melt duration should be limited: the remelting of the phosphate glass with the composition $50P_2O_5$–$40SrO$-$10Na_2O$ (in mol%) with the $SrAl_2O_4:Eu^{2+},Dy^{3+}$ phosphors with a diameter of ~40–50 μm should be no longer than 7 min. Because of the micrometer size of the phosphors, it was not possible to draw fiber below a diameter of about 400 μm. Despite the presence of PeL microparticles in the fiber, 7 cm of the fiber can be excited when UV light is injected into the fibers. Finally, the addition of the phosphors into the bioactive glass was demonstrated to have no significant impact on the ability of the glass to resorb and to promote the formation of a reactive layer. Despite the formation of this reactive layer, the fibers still exhibit visible green afterglow clearly showing that the obtained results are promising toward the processing of biophotonic fibers with

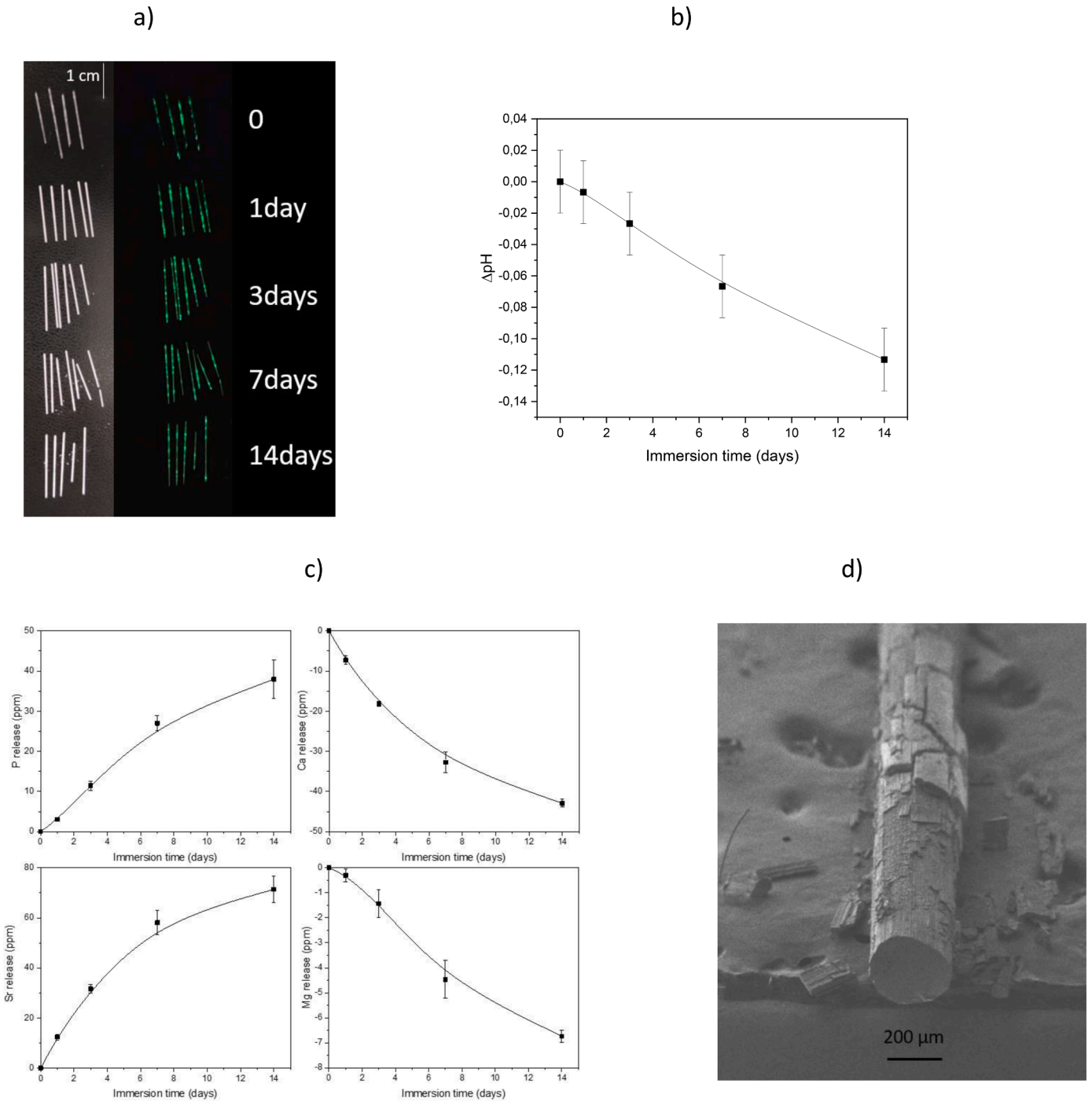

Fig. 6. Pictures in daylight and after stopping the UV irradiation of the fibers after immersion in SBF for up to 14 days (a). Change in pH (respective to the pH of the blank SBF) b) P, Ca, Sr and Mg release in SBF solution for up to 10 days (c) SEM image of the fiber after 14 days in SBF (d).

Table 1
Compositional analysis of the fiber surface.

Element (%at) (±1%at)	O	Na	Mg	P	Cl	K	Ca	Al	Sr
Theoretical composition	65	4	0	22	0	0	0	0	9
After 14 days in SBF	47	1	2.7	20.4	0.7	0.3	15.5	0.2	12.2

persistent luminescence.

CRediT authorship contribution statement

L.P. conceived and designed this work. A.L. and B.B. prepared and characterized the preforms and fibers. S.V. and M.L. carried out the

spectroscopic measurement of the materials with persistent luminescence. T.W.H and J.B drew the fibers. A.S and J.M. studied the bioresponse of the fibers. All authors discussed the results and contributed to the writing of the manuscript.

Declaration of Competing Interest

The authors declare that they have no known competing financial interests or personal relationships that could have appeared to influence the work reported in this paper.

Acknowledgement

The authors would like to acknowledge Academy of Finland (Flagship Programme, Photonics Research and Innovation PREIN-320165 and Academy Projects −326418, 328077, 331924, 328078 and 328079). JM would also like to acknowledge the Jane and Aatos Erkko Foundation. BB would also like to acknowledge the Polish National Agency for Academic Exchange (Bekker program, project PPN/BEK/2020/1/00074). JB and TWH acknowledge the J. E. Sirrine Foundation. This work made use of Tampere Microscopy Center facilities at Tampere University.

References

[1] L.L. Hench, R.J. Splinter, W.C. Allen, T.K. Greenlee, J. Biomed, Mater. Res. 5 (6) (1971) 117–141.
[2] P. Wang, Y. Semenova, G.Farrell Q.Wu, Microw. Opt. Technol. Lett. 52 (2010) 2231.
[3] V.V. Välimäki, N. Moritz, J.J. Yrjans, M. Dalstra, H.T. Aro, Biomater. 26 (2005) 6693–6703.
[4] J. Rao, A. Dragulescu-Andrasi, H. Yao, Curr. Opin. Biotechnol. 18 (2007) 17.
[5] Q. le Masne de Chermon, C. Chanéac, J. Seguin, F. Pellé, S. Maîtrejean, J.-.P. Jolivet, D. Gourier, M. Bessodes, D. Scherman, Proc. Natl. Acad. Sci. U.S.A. 104 (2007) 9266.
[6] T. Aitasalo, J. Hölsä, H. Jungner, M. Lastusaari, J. Niittykoski, J. Phys. Chem B. 110 (2006) 4589.
[7] K. Van den Eeckhout, P.F. Smet, D. Poelman, Mater. 3 (2010) 2536–2566.
[8] T. Nakanishi, Y. Katayama, J. Ueda, T. Honma, S. Tanabe, T. Komatsu, J. Ceram. Soc. Jpn. 119 (2011) 609–615.
[9] J. Zhao, X. Zheng, E.P. Schartner, P. Ionescu, R. Zhang, T.-.L. Nguyen, D. Jin, H. Ebendorff-Heidepriem, Adv. Opt. Mater. 4 (2016) 1507–1517.
[10] N. Ojha, H. Nguyen, T. Laihinen, T. Salminen, M. Lastusaari, L. Petit, Corros. Sci. 135 (2018) 207.
[11] N. Ojha, T. Laihinen, T. Salminen, M. Lastusaari, L. Petit, Ceram. Int. 44 (2018) 11807–11811.
[12] M. Hasnat, V. Lahti, H. Byron, M. Lastusaari, L. Petit, Scr. Mater. 199 (2021), 113864.
[13] L.L. Hench, Ö.H. Andersson, Bioactive Glasses. In: An Introduction to Bioceramics, June Wilson (1993).
[14] Ö.H. Andersson, K.H. Karlsson, Advance in Biomaterials No 8 (1990). Elsevier (Amsterdam).
[15] J. Massera, S. Fagerlund, L. Hupa, M. Hupa, J. Am. Ceram. Soc. 95 (2012) 607–613.
[16] J. Clement, J.M. Manero, J.A. Planell, J. Mater. Sci. Mater. Med. 10 (1999) 729–732.
[17] J.C. Knowles, J. Mater. Chem. 13 (2003) 2395–2401.
[18] L. Muñoz-Senovilla, F. Muñoz, G. Tricot, I. Ahmed, A.J. Parsons, J. Mater. Sci. 52 (2017) 9166–9178.
[19] P. Lopez-Iscoa, N. Ohja, D. Pugliese, A. Mishra, R. Gumenyuk, N.G. Boetti, D. Janner, J. Troles, B. Bureau, C. Boussard-Plédel, J. Massera, D. Milanese, L. Petit, J. Am. Ceram. Soc. 102 (2019) 6882–6892.
[20] A. Lapa, M. Cresswell, P. Jackson, A.R. Boccaccini, Adv. Appl. Ceram. 119 (2020) 1–14.
[21] C. Vitale-Brovarone, G. Novajra, D. Milanese, J. Lousteau, J.C. Knowles, Mater. Sci. Eng. C. 31 (2) (2011) 434–442.
[22] J. Massera, I. Ahmed, L. Petit, V. Aallos, L. Hupa, Mater. Sci. Eng. C. 37 (2014) 251–257.
[23] T. Kokubo, H. Kushitani, S. Sakka, T. Kitsugi, T. Yamamuro, J. Biomed. Mater. Res. 24 (1990) 721–734.
[24] J. Massera, M. Mayran, J. Rocherullé, L. Hupa, J. Mater. Sci. 50 (2015) 3091–3102.
[25] V. Lahti, N. Ojha, S. Vuori, M. Lastusaari, L. Petit, Mater. Chem. Phys. 274 (2021), 125164.
[26] T. Aitasalo, J. Hölsä, H. Jungner, J.-.C. Krupa, M. Lastusaari, J. Legendziewicz, J. Niittykoski, Radiat. Meas. 38 (2004) 727–730.
[27] J. Massera, M. Gaussiran, P. Głuchowski, M. Lastusaari, L. Hupa, L. Petit, J. Eur. Ceram. Soc. 35 (14) (2015) 3863–3871.
[28] J. Massera, L. Petit, T. Cardinal, J.J. Videau, M. Hupa, L. Hupa, J. Mater. Sci. Mater. Med. 24 (2013) 1407–1416.
[29] J. Massera, L. Hupa, J. Mater. Sci. Mater. Med. 25 (2014) 657–668.